ACS Macro Letters

pubs.acs.org/macroletters Letter

Bottlebrush Midblocks Promote Colloidal Bridging of Telechelic Polymers

Daniel P. Keane, Timea Kolozsvary, Benjamin McDonald,* and Ryan Poling-Skutvik*

Cite This: ACS Macro Lett. 2024, 13, 1304−1310 Read Online

ACCESS | Metrics & More | Article Recommendations | Supporting Information

ABSTRACT: Telechelic polymers are effective rheological modifiers that bridge between associative constituents to form elastic networks. The performance of linear telechelic chains, however, is controlled by entropic forces and thus suffers from an upper limit on bridge formation. This work overcomes this limitation by utilizing telechelic triblock copolymers containing bottlebrush midblocks. By comparing the rheological properties of emulsions linked by telechelic bottlebrush polymers to those containing linear chains, we determined that telechelic polymers with bottlebrush midblocks form elastic networks more efficiently. These enhanced rheological properties arise from the high stiffness of the bottlebrush midblocks, which offsets the entropic stretching penalty for bridge formation, enabling them to more readily form networks. This molecular-level control over polymer conformation in complex fluids opens avenues for designing highly elastic networks with minimal polymeric additives.

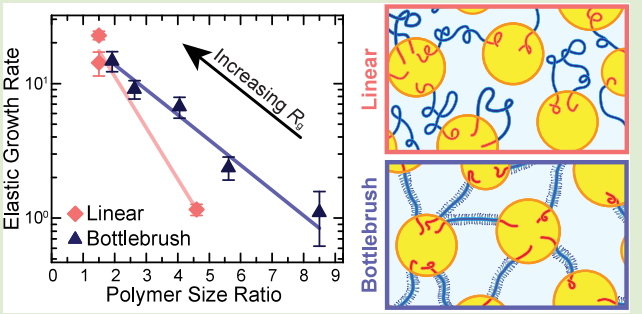

Telechelic polymers contain reactive or associative endgroups that facilitate their self-assembly in melts,[1−4] in solution,[5−11] and in the presence of constituents such as colloidal suspensions[12−15] or emulsions.[16−20] This self-assembly depends on both solvent choice and polymer molecular weight M_w. When dispersed in a midblock-selective solvent, the endgroups of telechelic polymers can associate with themselves to micellize[7,9,10,21] or with neighboring chains to form a network.[5,11,22] Network formation can be enhanced through the inclusion of associative constituents, such as colloids or emulsions,[20,23,24] in which the functional endgroups of the telechelic chains enthalpically associate with the particle surfaces or partition into dispersed droplets, while the midblock remains in the continuous phase. Each chain will thus adopt one of two conformations: a loop with both endgroups coordinating with the same constituent particle or a bridge with each endgroup coordinating with a distinct particle. Because loops serve as defects,[25,26] the properties of the resulting network depend on the ratio at which the polymers form bridges versus loops. In contrast to block copolymer melts where structure emerges from geometric constraints and evolves thermodynamically,[27,28] the structure of suspensions is dictated by the constituent size and volume fraction. Thus, there remain open questions of how telechelic block copolymers couple to this amorphous structure and how control over this interplay can drive the system to a highly bridged state by minimizing loop formation.

Telechelic polymers with low molecular weight M_{end} endblocks form viscoelastic networks in colloidal systems[19,29−31] because the weak associations exist in a dynamic equilibrium that facilitates relaxations.[32,33] Alternatively, chains with large M_{end} generate highly elastic gels because the endblocks irreversibly associate, forming kinetically trapped systems that resist thermal fluctuations.[20,24] While M_{end} controls network relaxations, midblock M_w (M_{mid}) controls the bridging fraction $\varepsilon = n_B/n_T$, where n_B and n_T are the number densities of bridging chains and total chains, respectively. Previous simulation work on polymer-linked colloids has shown that bridging is entropically controlled according to the ratio of the surface-to-surface distance D_{ID} to midblock radius of gyration $R_{g,mid}$.[34−36] At a large D_{ID} or small $R_{g,mid}$, polymers must undergo entropically unfavorable stretching to interact with neighboring particles and therefore preferentially adopt loop conformations. By contrast, for small D_{ID} or large $R_{g,mid}$, the chains require only minor deformations to interact with neighboring particles, and the bridging becomes governed by the statistical probability. As $D_{ID}/R_{g,mid} \rightarrow 0$, ε approaches a maximum of approximately 1/3, arising from the statistics of there being two independent combinations to form a loop but only one to form a bridge, which presents a significant limitation on the use of telechelic polymers as rheological modifiers.

Received: June 21, 2024
Revised: August 13, 2024
Accepted: September 10, 2024

https://doi.org/10.1021/acsmacrolett.4c00428
ACS Macro Lett. 2024, 13, 1304−1310

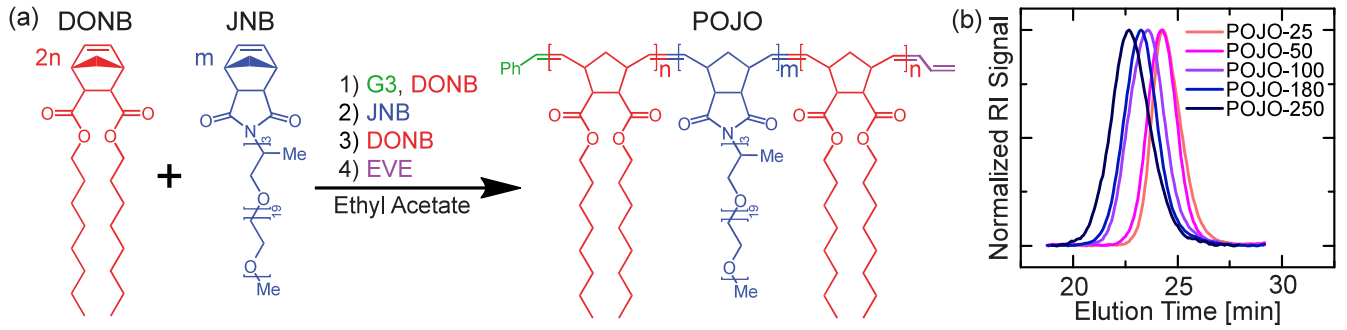

Figure 1. (a) Synthesis scheme of the POJO telechelic triblock copolymer from dioctyl dicarboxylic norbornene (DONB) and Jeffamine M-1000 norbornene (JNB). (b) Normalized refractive index (RI) signal as a function of elution time for POJO with varying M_{mid}.

In this Letter, we improve the bridging efficiency by introducing an entropic penalty for loop formation through the use of telechelic triblock copolymers with bottlebrush midblocks. The pendant sidechains of bottlebrush polymers introduce steric hindrance along the backbone, increasing the midblock persistence length[37−39] and spatially separating the endblocks. The size and rigidity of bottlebrush polymers depends on the degree of polymerization of both the backbone N_{bb} and sidechains N_{sc} as well as the sidechain grafting density.[38,40−57] Here, we synthesize telechelic triblock copolymers with bottlebrush midblocks and linear endblocks through ring-opening metathesis polymerization (ROMP) to create a library of polymers with varying M_{mid} and constant M_{end}. We use these copolymers to link emulsions into elastic networks, and by comparing the dependence of emulsion elasticity on the normalized length scale $D_{ID}/R_{g,mid}$, we find that polymers with bottlebrush midblocks exhibit a quantitatively higher relative bridging fraction ε compared with those with linear midblocks. Our findings demonstrate that by tailoring polymer topology, we can modify the coupling of polymer conformation to the structure of complex fluids, resulting in highly bridged, elastic networks.

The polymer-linked emulsions (PLEs) must satisfy two key criteria. First, the continuous and dispersed phases must be immiscible and minimally volatile. Second, the telechelic triblock copolymers must have orthogonally soluble blocks such that the endblocks partition into the oil droplets and the midblocks into the continuous phase. To satisfy these requirements, we use ROMP to synthesize triblock copolymers containing hydrophobic poly(dioctyl dicarboxylic norbornene) endblocks[58] and bottlebrush midblocks of poly(Jeffamine M-1000 norbornene)[59] − a norbornene group functionalized with a hydrophilic polyetheramine of $N_{sc} \approx 22$ with repeating units of propylene oxide and ethylene oxide (Figure 1a). Based on established scaling laws,[60] we estimate that the Jeffamine M-1000 side chains have a radius of gyration $R_g \approx 1$ nm, leading to a persistence length $l_p \approx 2R_g \approx 2$ nm.[37,61] The synthesis employs a one-pot ROMP procedure[62] initiated by Grubb's third generation catalyst[63] (G3) with the sequential addition of macromonomers and termination by ethyl vinyl ether (EVE). M_{end} is held constant at 34 ± 5 kDa to achieve effectively irreversible endblock partitioning,[20,24] and M_{mid} is varied from 25 to 250 kDa (equivalent to $N_{bb} \approx 21-210$) to test midblocks with conformations ranging from star-like ($N_{bb} \approx N_{sc}$) to worm-like chains ($N_{bb} \gg N_{sc}$).[48] Furthermore, there is a practical upper limit on M_{mid} because of the challenges in losing catalyst activity from monomer coordination or residual impurities. The M_w and dispersity $Đ$ of the poly(dioctyl dicarboxylic norbornene)-*b*-poly(Jeffamine M-1000 norbornene)-*b*-poly(dioctyl dicarboxylic norbornene) (POJO) triblock copolymers are detailed in Table 1, and GPC elution curves are shown in Figure 1b. Additional synthesis details are provided in the Supporting Information. The POJO polymers were added to 1-decanol-in-water emulsions at nominal concentrations of 0.25 to 3 wt %, corresponding to molar concentrations ranging from 0.012 to 0.48 mmol/L depending on M_{mid}. Specific concentrations are detailed in the Supporting Information. At concentrations above ∼3 wt %, samples appear heterogeneous as a result of polymer insolubility or insufficient mixing, setting an upper bound for the testable concentrations. The emulsions have droplet diameters d_H = 400 nm, as determined by DLS (Supporting Information) and a volume fraction ϕ = 0.5. Rheological properties are characterized on a TA Instruments HR-20 Rheometer using 2° cone-and-plate geometries with diameters of 20 and 60 mm, respectively, and a gap height of 54 μm.

Table 1. Polymer Nomenclature, Target Weight-Average Molecular Weight M_w of the Midblock and Endblocks, Total Measured M_w, and Measured Dispersity $Đ$ of the POJO Polymers

polymer	target midblock M_w (kDa)	target endblocks M_w (kDa)	total M_w (kDa)	$Đ$
POJO-25	25	30	80.7	1.36
POJO-50	50	30	97.8	1.31
POJO-100	100	30	176.5	1.45
POJO-180	180	30	218.8	1.58
POJO-250	250	30	332.0	1.74

We characterize the PLE rheology as a function of both oscillation amplitude γ and oscillation frequency ω (Figure 2). While the neat emulsions are dominated by liquid-like behavior (Supporting Information), we observe a dramatic increase in emulsion elasticity upon the addition of POJO, with dependencies on both polymer concentration c and M_{mid}. The PLEs are elastic in the linear viscoelastic region (i.e., $\gamma \lesssim 0.6\%$) with the storage modulus G' greater than the loss modulus G'', and they exhibit the typical signs of yielding for Type III materials[64] as γ is further increased, with the appearance of a maximum in G'', a crossover between G' and G'', and a subsequent decay in both moduli (Figure 2a). PLEs with higher c or M_{mid} typically display greater moduli and larger overshoots in G'',[65−67] suggesting that increased n_B promotes the formation of more cohesive elastic networks.

We additionally examined the system through linear frequency sweeps, measuring G' and G'' as a function of ω

https://doi.org/10.1021/acsmacrolett.4c00428
ACS Macro Lett. 2024, 13, 1304−1310

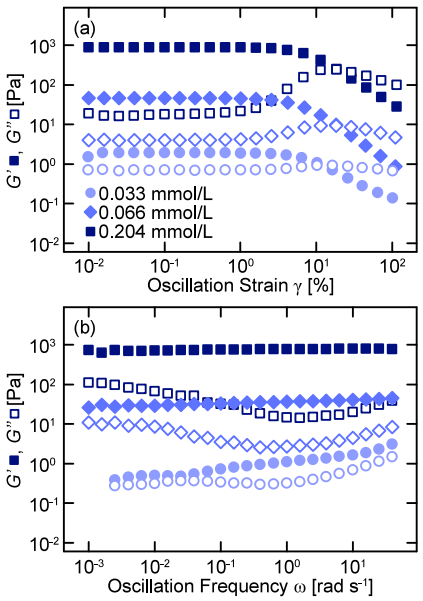

Figure 2. Storage modulus G' (closed) and loss modulus G'' (open) as a function of (a) strain amplitude γ at a fixed frequency ω = 10 rad s^{-1} and (b) as a function of frequency ω at a fixed amplitude γ = 0.3% for emulsions containing POJO-180 of varying concentrations c.

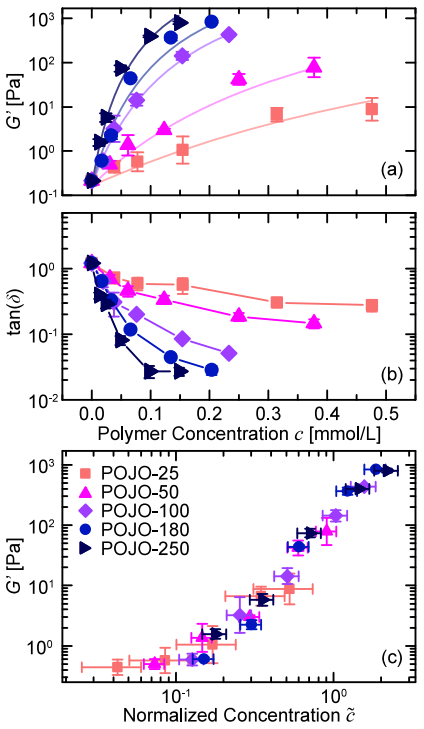

Figure 3. (a) Storage modulus G' and (b) loss tangent tan(δ) as a function of polymer concentration c at ω = 10 rad s^{-1}. Curves in (a) are fits to eq 1 and in (b) are guides to the eye. (c) Storage modulus G' as a function of normalized polymer concentration $\tilde{c} = mc$. Error bars in y are one log-normal standard deviation, and error bars in x are 95% confidence intervals on the fitting parameter m.

(Figure 2b). For nearly all c and M_{mid}, the PLEs are elastic with $G' > G''$ across all experimentally accessible ω. Furthermore, G' becomes nearly independent from ω at higher c, characteristic of soft, glassy materials[68,69] and indicating that large-scale viscous rearrangements are suppressed. This glassy-like rheology is further supported by the presence of a minimum in G'' centered at $\omega \approx 1$ rad s^{-1}. The upturn in G'' at higher frequencies reflects contributions from rapid relaxations of individual polymer segments,[70] and the increase at lower frequencies corresponds to slow structural relaxations. Unlike standard Maxwellian descriptions of viscoelasticity,[71,72] G' and G'' do not display a crossover even as ω approaches 10^{-3} rad s^{-1}, demonstrating that the endblocks are strongly partitioned into the dispersed droplets and kinetically trapped by enthalpic forces. We observe qualitatively similar frequency and concentration dependencies regardless of M_{mid}, with decreasing M_{mid} resulting in similar effects as decreasing c (Supporting Information).

To further explore the network formation of the telechelic bottlebrushes, we examined the PLE elasticity at a fixed frequency ω = 10 rad s^{-1} as a function of c (Figure 3). For all M_{mid}, increasing c leads to larger G' and smaller tan(δ) = G''/G' due to a greater bridging density n_B. Polymers with larger M_{mid} form cohesive networks more rapidly, consistent with earlier findings on linear telechelic polymers.[20,35,36] Although both linear and bottlebrush telechelic polymers produce elastic networks, PLEs formed by linear polymers[20] display a plateau at tan(δ) $\approx 10^{-1}$ whereas the bottlebrush PLEs approach tan(δ) $\approx 10^{-2}$ at the highest c and M_{mid}. These low values of tan(δ) suggest that the POJO chains contribute more specifically to network elasticity with minimal viscous dissipation, which may result from fewer relaxation modes in the bottlebrush midblocks.

These rheological dependencies on c can be quantified by fitting each curve to a modified Langmuir isotherm, given by

$$G = G_0 \exp\left(\frac{Kmc}{1 + mc}\right) \quad (1)$$

where G_0 = 0.16 ± 0.02 Pa is the storage modulus of the neat emulsion, K is a constant related to the elasticity of the emulsion at the high-c plateau, and m characterizes the increase in emulsion elasticity per mole of polymer in the low-c limit. We assume that network properties at infinite c are controlled by the size and volume fraction of the emulsion droplets and therefore restrict K to be constant across the samples. A global fit on K finds K = 13.0 ± 0.7, corresponding to a limiting plateau $G' = G_0 \exp(K) \approx 70$ kPa. Although largely empirical, this fit successfully captures the initial exponential increase and eventual plateau in elasticity across all c and M_{mid}. By defining a normalized concentration $\tilde{c} = cm$, we collapse G' onto a master curve for all M_{mid} (Figure 3c), demonstrating that the mechanisms by which these telechelic polymers form networks is preserved across all M_{mid}. We hypothesize that the sigmoidal growth in elasticity (Figure 3c) emerges from an interplay of physical phenomena, as follows: (1) the plateau in G' at low $\tilde{c}$ corresponds to the finite elasticity of the neat emulsion, (2) the rise in G' occurs as bridging chains induce percolation between droplets,[14,73−76] and (3) the high-$\tilde{c}$ plateau in G' arises as polymers saturate the droplet surfaces and begin to form redundant bridges. A precise theoretical description of these physics, however, remains elusive due to the challenging physics of this system. Because the interaction range in PLEs is on the order of $R_{g,mid}$, the PLE system violates the assumption underlying existing theories for suspensions of attractive colloids that the interaction range is significantly smaller than the particle size.[77−79] Furthermore, mean-field theories, such as

https://doi.org/10.1021/acsmacrolett.4c00428
ACS Macro Lett. 2024, 13, 1304−1310

the affine network model,[71] severely underestimate the moduli of these PLEs, which we attribute to the heterogeneous structure of the system. Additional theoretical advances are therefore needed to mechanistically describe these complex systems beyond our empirical model.

Nevertheless, this empirical fit provides a framework to describe the elastic growth by quantifying the initial rate of change in G' in a single parameter m. We posit that m captures the increase in elasticity per chain, which is directly proportional to the product of the bridging fraction and strength of endblock partitioning[20] according to $m \sim \varepsilon \mathcal{F}(M_{end})$. Therefore, telechelic polymers with different endblocks are expected to have different values for $\mathcal{F}(M_{end})$ but similar dependencies on m. To isolate contributions from ε, we quantify the dependence of m on the normalized distance $D_{ID}/R_{g,mid}$ for telechelic chains with either bottlebrush or linear midblocks (Figure 4), where $D_{ID} = d_H[(\phi_{max}/\phi)^{1/3}-1] \approx$

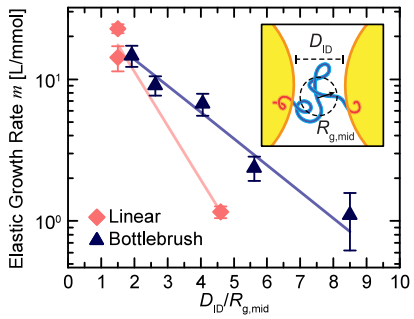

Figure 4. Elastic growth rate m as a function of the ratio of interdroplet distance to midblock radius of gyration $D_{ID}/R_{g,mid}$ for POJO (this work) and SEOS (ref 20) polymers. Curves are exponential fits. Inset: Schematic illustrating D_{ID} and $R_{g,mid}$.

34 nm is the surface-to-surface distance between droplets,[80] $\phi_{max} = 0.64$ corresponds to random close packing, and $R_{g,mid}$ is the radius of gyration of homopolymers of the midblock determined from intrinsic viscosity measurements (Supporting Information). For both systems, we observe that m decreases exponentially with increasing $D_{ID}/R_{g,mid}$ according to $m \sim \exp(-aD_{ID}/R_{g,mid})$, where a characterizes the decay rate. For linear polymers, $a = 0.93 \pm 0.10$, while for bottlebrush polymers, $a = 0.44 \pm 0.05$. By comparing the decay rates a rather than m, we remove effects arising from the different endblock chemistries to quantify the effect of the normalized distance on the bridging fraction ε. For example, we identify that for linear polymers, m decays over an order of magnitude from $D_{ID}/R_{g,mid} \approx 1$ to 4.7 whereas in bottlebrush systems, m decreases a similar amount only when $D_{ID}/R_{g,mid} \approx 8.5$. This difference in bridging propensity over larger distances indicates that the high stiffness of the bottlebrush midblock and subsequent spatial separation of the endblocks enhance bridge formation and prevent the dramatic decline in elasticity observed for linear polymers. While a provides insight into the decay rate of the bridging fraction, we cannot comment on the exact values of ε in each system. To the best of our knowledge, no experimental technique can currently distinguish between bridging and looping chains in these classes of complex fluids, despite previous observations in polymer networks,[81] solutions,[82] suspensions,[83] and melts.[4,84−88] Thus, resolving even relative bridging densities solves a critical knowledge gap in polymer physics and enables direct comparisons of the efficacy of different polymer chemistries and topologies.

We also note that this normalization $D_{ID}/R_{g,mid}$ already accounts for the larger sizes of bottlebrush polymers at comparable degrees of polymerization, and thus, the enhanced bridging of bottlebrushes is not simply a size effect. Instead, we attribute this enhanced bridging capability to two primary mechanisms. First, the longer persistence length of the bottlebrush midblocks ($l_p \approx 2$ nm) introduces an entropic penalty for loop formation. Second, the worm-like nature of the chains leads to spatially localized endblocks, quantified by a nonzero average end-to-end vector.[89] Although the large persistence lengths and worm-like chain behavior of bottlebrush polymers have been well-established in the literature, the effects of these conformational characteristics on the bridging behavior in colloidal systems have not been explored. In melts, triblock bottlebrush polymers can readily form loops as they orient parallel to interfaces, even decreasing the bridging fraction relative to linear polymers.[4,90] This melt behavior contrasts with the behavior of telechelic bottlebrushes in suspensions observed here, which we attribute to length scales in suspensions being set by particle size and volume fraction rather than by the relative fractions of each block. Additionally, phase separation proceeds thermodynamically in a melt, but partitioning is primarily controlled by the kinetics in these emulsions. We expect that this combination of kinetically controlled association and coupling between the polymer conformation and emulsion structure plays a dominant role in the enhanced bridging fraction achieved by bottlebrush midblocks.

Our work demonstrates that telechelic triblock copolymers are effective rheological modifiers, capable of bridging between emulsion droplets to form elastic networks. We synthesized triblock copolymers with bottlebrush midblocks at different degrees of polymerization via ROMP, and we utilized these polymers to assemble emulsions into elastic networks. The resulting polymer-linked emulsions display unique rheological behavior with suppressed terminal relaxations and high elasticities that can be collapsed onto a single master curve according to the elastic growth rate m. Although the exponential scaling of elasticity does not follow existing theoretical predictions, we show that this growth rate m is directly related to the bridging fraction ε and facilitates a quantitative comparison of bridging between different polymer chemistries. We observe significantly greater bridge formation for bottlebrush midblocks than for linear midblocks, indicating that stiffer midblocks promote bridging by imposing an entropic penalty for loop formation and spatially separating endblocks. Our results suggest that modulating the structure and conformations of telechelic block copolymers is a promising approach to tune their bridging ability. This demonstrated control opens a broad swath of opportunities to design dynamic complex fluids that can improve processability and performance in advanced manufacturing,[91] respond to environmental stimuli to drive controlled transport,[23] or exhibit biomimetic properties for tissue engineering and biomanufacturing.[92]

■ ASSOCIATED CONTENT

Supporting Information

The Supporting Information is available free of charge at https://pubs.acs.org/doi/10.1021/acsmacrolett.4c00428.

https://doi.org/10.1021/acsmacrolett.4c00428
ACS Macro Lett. 2024, 13, 1304−1310

Experimental section, intrinsic viscosity measurements, synthesis details, polymer and emulsion details, neat emulsion characterization, additional rheological data, information on fitting methods, and calculations (PDF)

AUTHOR INFORMATION

Corresponding Authors

Benjamin McDonald − *Department of Chemistry, Brown University, Providence, Rhode Island 02912, United States;* orcid.org/0000-0002-2408-2448; Email: benjamin_mcdonald1@brown.edu

Ryan Poling-Skutvik − *Department of Chemical Engineering, University of Rhode Island, Kingston, Rhode Island 02881, United States;* orcid.org/0000-0002-1614-1647; Email: ryanps@uri.edu

Authors

Daniel P. Keane − *Department of Chemical Engineering, University of Rhode Island, Kingston, Rhode Island 02881, United States*

Timea Kolozsvary − *Department of Chemistry, Brown University, Providence, Rhode Island 02912, United States*

Complete contact information is available at: https://pubs.acs.org/10.1021/acsmacrolett.4c00428

Author Contributions

CRediT: **Daniel P. Keane** conceptualization, data curation, formal analysis, investigation, methodology, validation, writing - original draft, writing - review & editing; **Timea Kolozsvary** methodology, writing - review & editing; **Benjamin McDonald** conceptualization, funding acquisition, project administration, resources, supervision, writing - review & editing; **Ryan Poling-Skutvik** conceptualization, funding acquisition, project administration, resources, supervision, writing - original draft, writing - review & editing.

Notes

The authors declare no competing financial interest.

ACKNOWLEDGMENTS

This research was supported by the National Science Foundation (CBET-2339052) (D.K. and R.P.-S.). B.R.M. and T.K. gratefully acknowledge support from Rhode Island Institutional Development Award (IDeA) Network of Biomedical Research Excellence from the National Institute of General Medical Sciences of the National Institutes of Health under Grant Number P20GM103430, Sub-Award No.: 0009701/07152022A.

REFERENCES

(1) Matsen, M. W.; Schick, M. Lamellar Phase of a Symmetric Triblock Copolymer. *Macromolecules* **1994**, *27*, 187−192.

(2) Matsen, M. W. Equilibrium Behavior of Asymmetric ABA Triblock Copolymer Melts. *J. Chem. Phys.* **2000**, *113*, 5539−5544.

(3) Keith, A. N.; Vatankhah-Varnosfaderani, M.; Clair, C.; Fahimipour, F.; Dashtimoghadam, E.; Lallam, A.; Sztucki, M.; Ivanov, D. A.; Liang, H.; Dobrynin, A. V.; Sheiko, S. S. Bottlebrush Bridge between Soft Gels and Firm Tissues. *ACS Cent. Sci.* **2020**, *6*, 413−419.

(4) Nian, S.; Cai, L.-H. Dynamic Mechanical Properties of Self-Assembled Bottlebrush Polymer Networks. *Macromolecules* **2022**, *55*, 8058−8066.

(5) Nguyen-Misra, M.; Mattice, W. L. Micellization and Gelation of Symmetric Triblock Copolymers with Insoluble End Blocks. *Macromolecules* **1995**, *28*, 1444−1457.

(6) Laurer, J. H.; Khan, S. A.; Spontak, R. J.; Satkowski, M. M.; Grothaus, J. T.; Smith, S. D.; Lin, J. S. Morphology and Rheology of SIS and SEPS Triblock Copolymers in the Presence of a Midblock-Selective Solvent. *Langmuir* **1999**, *15*, 7947−7955.

(7) Nardin, C.; Hirt, T.; Leukel, J.; Meier, W. Polymerized ABA Triblock Copolymer Vesicles. *Langmuir* **2000**, *16*, 1035−1041.

(8) Vega, D. A.; Sebastian, J. M.; Loo, Y.-L.; Register, R. A. Phase Behavior and Viscoelastic Properties of Entangled Block Copolymer Gels. *J. Polym. Sci. B Polym. Phys.* **2001**, *39*, 2183−2197.

(9) Lu, J.; Bates, F. S.; Lodge, T. P. Remarkable Effect of Molecular Architecture on Chain Exchange in Triblock Copolymer Micelles. *Macromolecules* **2015**, *48*, 2667−2676.

(10) Zinn, T.; Willner, L.; Knudsen, K. D.; Lund, R. Self-Assembly of Mixtures of Telechelic and Monofunctional Amphiphilic Polymers in Water: From Clusters to Flowerlike Micelles. *Macromolecules* **2017**, *50*, 7321−7332.

(11) Badani Prado, R. M.; Mishra, S.; Ahmed, H.; Burghardt, W. R.; Kundu, S. Temperature- and Strain-Dependent Transient Microstructure and Rheological Responses of Endblock-Associated Triblock Gels of Different Block Lengths in a Midblock Selective Solvent. *Soft Matter* **2022**, *18*, 7020−7034.

(12) Wang, S.; Larson, R. G. Multiple Relaxation Modes in Suspensions of Colloidal Particles Bridged by Telechelic Polymers. *J. Rheol.* **2018**, *62*, 477−490.

(13) Zhang, W.; Travitz, A.; Larson, R. G. Modeling Intercolloidal Interactions Induced by Adsorption of Mobile Telechelic Polymers onto Particle Surfaces. *Macromolecules* **2019**, *52*, 5357−5365.

(14) Song, J.; Rizvi, M. H.; Lynch, B. B.; Ilavsky, J.; Mankus, D.; Tracy, J. B.; McKinley, G. H.; Holten-Andersen, N. Programmable Anisotropy and Percolation in Supramolecular Patchy Particle Gels. *ACS Nano* **2020**, *14*, 17018−17027.

(15) Krishnamurthy, S.; Parthasarathy, G.; Larson, R. G.; Mani, E. Brownian Dynamics Simulations of Telechelic Polymer - Latex Suspensions under Steady Shear. *Soft Matter* **2023**, *19*, 2949−2961.

(16) Odenwald, M.; Eicke, H.-F.; Meier, W. Transient Networks by ABA Triblock Copolymers and Microemulsions: A Rheological Study. *Macromolecules* **1995**, *28*, 5069−5074.

(17) Barnes, T. J.; Prestidge, C. A. PEO-PPO-PEO Block Copolymers at the Emulsion Droplet-Water Interface. *Langmuir* **2000**, *16*, 4116−4121.

(18) Sarraguça, J. M. G.; Pais, A. A. C. C.; Linse, P. Structure of Microemulsion-ABA Triblock Copolymer Networks. *Langmuir* **2008**, *24*, 11153−11163.

(19) Malo De Molina, P.; Appavou, M.-S.; Gradzielski, M. Oil-in-Water Microemulsion Droplets of TDMAO/Decane Interconnected by the Telechelic C_{18}-EO_{150}-C_{18}: Clustering and Network Formation. *Soft Matter* **2014**, *10*, 5072−5084.

(20) Keane, D. P.; Mellor, M. D.; Poling-Skutvik, R. Responsive Telechelic Block Copolymers for Enhancing the Elasticity of Nanoemulsions. *ACS Appl. Nano Mater.* **2022**, *5*, 5934−5943.

(21) Meng, X.-X.; Russel, W. B. Structure and Size of Spherical Micelles of Telechelic Polymers. *Macromolecules* **2005**, *38*, 593−600.

(22) Tripathi, A.; Tam, K. C.; McKinley, G. H. Rheology and Dynamics of Associative Polymers in Shear and Extension: Theory and Experiments. *Macromolecules* **2006**, *39*, 1981−1999.

(23) Helgeson, M. E.; Moran, S. E.; An, H. Z.; Doyle, P. S. Mesoporous Organohydrogels from Thermogelling Photocrosslinkable Nanoemulsions. *Nat. Mater.* **2012**, *11*, 344−352.

(24) Keane, D. P.; Constantine, C. J.; Mellor, M. D.; Poling-Skutvik, R. Bridging Heterogeneity Dictates the Microstructure and Yielding Response of Polymer-Linked Emulsions. *Langmuir* **2023**, *39*, 7852−7862.

(25) Wang, J.; Wang, R.; Gu, Y.; Sourakov, A.; Olsen, B. D.; Johnson, J. A. Counting Loops in Sidechain-Crosslinked Polymers from Elastic Solids to Single-Chain Nanoparticles. *Chem. Sci.* **2019**, *10*, 5332−5337.

(26) Arora, A.; Lin, T.-S.; Beech, H. K.; Mochigase, H.; Wang, R.; Olsen, B. D. Fracture of Polymer Networks Containing Topological Defects. *Macromolecules* **2020**, *53*, 7346−7355.
(27) Bates, F. S.; Fredrickson, G. H. Block Copolymer Thermodynamics: Theory and Experiment. *Annu. Rev. Phys. Chem.* **1990**, *41*, 525−557.
(28) Bates, F. S.; Fredrickson, G. H. Block Copolymers−Designer Soft Materials. *Phys. Today* **1999**, *52*, 32−38.
(29) Tanaka, F.; Edwards, S. F. Viscoelastic Properties of Physically Crosslinked Networks. 1. Transient Network Theory. *Macromolecules* **1992**, *25*, 1516−1523.
(30) Meng, X.-X.; Russel, W. B. Rheology of Telechelic Associative Polymers in Aqueous Solutions. *J. Rheol.* **2006**, *50*, 189−205.
(31) Gonzalez, J. M.; Rodrigues, J. D. A.; Nascimento, R. S. V. ABA Low Molar Mass Triblock Copolymers in Reverse Emulsions: A Rheological Study. *J. Appl. Polym. Sci.* **2012**, *125*, 3282−3289.
(32) Hough, L. A.; Ou-Yang, H. D. Viscoelasticity of Aqueous Telechelic Poly(Ethylene Oxide) Solutions: Relaxation and Structure. *Phys. Rev. E* **2006**, *73*, 031802.
(33) Zinn, T.; Willner, L.; Lund, R. Telechelic Polymer Hydrogels: Relation between the Microscopic Dynamics and Macroscopic Viscoelastic Response. *ACS Macro Lett.* **2016**, *5*, 1353−1356.
(34) Misra, S.; Mattice, W. L. Telechelic Polymers between Two Impenetrable Adsorbing Surfaces. *Macromolecules* **1994**, *27*, 2058−2065.
(35) Puech, N.; Mora, S.; Testard, V.; Porte, G.; Ligoure, C.; Grillo, I.; Phou, T.; Oberdisse, J. Structure and Rheological Properties of Model Microemulsion Networks Filled with Nanoparticles. *Eur. Phys. J. E* **2008**, *26*, 13.
(36) Testard, V.; Oberdisse, J.; Ligoure, C. Monte Carlo Simulations of Colloidal Pair Potential Induced by Telechelic Polymers: Statistics of Loops and Bridges. *Macromolecules* **2008**, *41*, 7219−7226.
(37) Cai, L.-H.; Kodger, T. E.; Guerra, R. E.; Pegoraro, A. F.; Rubinstein, M.; Weitz, D. A. Soft Poly(Dimethylsiloxane) Elastomers from Architecture-Driven Entanglement Free Design. *Adv. Mater.* **2015**, *27*, 5132−5140.
(38) Paturej, J.; Sheiko, S. S.; Panyukov, S.; Rubinstein, M. Molecular Structure of Bottlebrush Polymers in Melts. *Sci. Adv.* **2016**, *2*, e1601478.
(39) Abbasi, M.; Faust, L.; Wilhelm, M. Comb and Bottlebrush Polymers with Superior Rheological and Mechanical Properties. *Adv. Mater.* **2019**, *31*, 1806484.
(40) Lecommandoux, S.; Chécot, F.; Borsali, R.; Schappacher, M.; Deffieux, A.; Brûlet, A.; Cotton, J. P. Effect of Dense Grafting on the Backbone Conformation of Bottlebrush Polymers: Determination of the Persistence Length in Solution. *Macromolecules* **2002**, *35*, 8878−8881.
(41) Rathgeber, S.; Pakula, T.; Wilk, A.; Matyjaszewski, K.; Beers, K. L. On the Shape of Bottle-Brush Macromolecules: Systematic Variation of Architectural Parameters. *J. Chem. Phys.* **2005**, *122*, 124904.
(42) Zhang, M.; Müller, A. H. E. Cylindrical Polymer Brushes. *J. Polym. Sci. A Polym. Chem.* **2005**, *43*, 3461−3481.
(43) Hsu, H.-P.; Paul, W.; Rathgeber, S.; Binder, K. Characteristic Length Scales and Radial Monomer Density Profiles of Molecular Bottle-Brushes: Simulation and Experiment. *Macromolecules* **2010**, *43*, 1592−1601.
(44) Liang, H.; Cao, Z.; Wang, Z.; Sheiko, S. S.; Dobrynin, A. V. Combs and Bottlebrushes in a Melt. *Macromolecules* **2017**, *50*, 3430−3437.
(45) Paturej, J.; Kreer, T. Hierarchical Excluded Volume Screening in Solutions of Bottlebrush Polymers. *Soft Matter* **2017**, *13*, 8534−8541.
(46) Pesek, S. L.; Xiang, Q.; Hammouda, B.; Verduzco, R. Small-Angle Neutron Scattering Analysis of Bottlebrush Backbone and Side Chain Flexibility. *J. Polym. Sci., Part B: Polym. Phys.* **2017**, *55*, 104−111.
(47) Chremos, A.; Douglas, J. F. A Comparative Study of Thermodynamic, Conformational, and Structural Properties of Bottlebrush with Star and Ring Polymer Melts. *J. Chem. Phys.* **2018**, *149*, 044904.
(48) Dutta, S.; Wade, M. A.; Walsh, D. J.; Guironnet, D.; Rogers, S. A.; Sing, C. E. Dilute Solution Structure of Bottlebrush Polymers. *Soft Matter* **2019**, *15*, 2928−2941.
(49) Jungmann, P.; Kreer, T.; Sommer, J.-U.; Paturej, J. Conformational Properties of End-Grafted Bottlebrush Polymers. *Macromolecules* **2021**, *54*, 161−169.
(50) Tang, Z.; Pan, X.; Zhou, H.; Li, L.; Ding, M. Conformation of a Comb-like Chain Free in Solution and Confined in a Nanochannel: From Linear to Bottlebrush Structure. *Macromolecules* **2022**, *55*, 8668−8675.
(51) Chen, G.; Dormidontova, E. E. Cyclic vs Linear Bottlebrush Polymers in Solution: Side-Chain Length Effect. *Macromolecules* **2023**, *56*, 3286−3295.
(52) Mai, X.; Hao, P.; Liu, D.; Ding, M. Conformation of a Comb-like Chain in Solution: Effect of Backbone Rigidity. *ACS Omega* **2023**, *8*, 11177−11183.
(53) Salinas-Soto, C. A.; Choe, Y.; Hur, S.-M.; Ramírez-Hernández, A. Exploring Conformations of Comb-like Polymers with Varying Grafting Density in Dilute Solutions. *J. Chem. Phys.* **2023**, *159*, 114901.
(54) Sunday, D. F.; Burns, A. B.; Martin, T. B.; Chang, A. B.; Grubbs, R. H. Relationship between Graft Density and the Dilute Solution Structure of Bottlebrush Polymers: An Inter-chemistry Comparison and Scaling Analysis. *Macromolecules* **2023**, *56*, 7419−7431.
(55) Zografos, A.; All, H. A.; Chang, A. B.; Hillmyer, M. A.; Bates, F. S. Star-to-Bottlebrush Transition in Extensional and Shear Deformation of Unentangled Polymer Melts. *Macromolecules* **2023**, *56*, 2406−2417.
(56) Chan, J. M.; Kordon, A. C.; Wang, M. Investigating the Effects of the Local Environment on Bottlebrush Conformations Using Super-Resolution Microscopy. *Nanoscale* **2024**, *16*, 2409−2418.
(57) Leo, C. M.; Jang, J.; Corey, E. J.; Neary, W. J.; Bowman, J. I.; Kennemur, J. G. Comparison of Polypentenamer and Polynorbornene Bottlebrushes in Dilute Solution. *ACS Polym. Au* **2024**, *4*, 235.
(58) Zuo, Y.-J.; Qu, J. How Does Aqueous Solubility of Organic Reactant Affect a Water-Promoted Reaction? *J. Org. Chem.* **2014**, *79*, 6832−6839.
(59) Ter Huurne, G. M.; Gillissen, M. A. J.; Palmans, A. R. A.; Voets, I. K.; Meijer, E. W. The Coil-to-Globule Transition of Single-Chain Polymeric Nanoparticles with a Chiral Internal Secondary Structure. *Macromolecules* **2015**, *48*, 3949−3956.
(60) Bailey, F. E.; Kucera, J. L.; Imhof, L. G. Molecular Weight Relations of Poly(Ethylene Oxide). *J. Polym. Sci.* **1958**, *32*, 517−518.
(61) Daniel, W. F. M.; Burdyńska, J.; Vatankhah-Varnoosfaderani, M.; Matyjaszewski, K.; Paturej, J.; Rubinstein, M.; Dobrynin, A. V.; Sheiko, S. S. Solvent-Free, Supersoft and Superelastic Bottlebrush Melts and Networks. *Nat. Mater.* **2016**, *15*, 183−189.
(62) Bielawski, C. W.; Grubbs, R. H. Living Ring-Opening Metathesis Polymerization. *Prog. Polym. Sci.* **2007**, *32*, 1−29.
(63) Sanford, M. S.; Love, J. A.; Grubbs, R. H. A Versatile Precursor for the Synthesis of New Ruthenium Olefin Metathesis Catalysts. *Organometallics* **2001**, *20*, 5314−5318.
(64) Hyun, K.; Kim, S. H.; Ahn, K. H.; Lee, S. J. Large Amplitude Oscillatory Shear as a Way to Classify the Complex Fluids. *J. Non-Newton. Fluid* **2002**, *107*, 51−65.
(65) Donley, G. J.; Singh, P. K.; Shetty, A.; Rogers, S. A. Elucidating the G″ Overshoot in Soft Materials. *Proc. Natl. Acad. Sci. U.S.A.* **2020**, *117*, 21945−21952.
(66) Kamani, K.; Donley, G. J.; Rogers, S. A. Unification of the Rheological Physics of Yield Stress Fluids. *Phys. Rev. Lett.* **2021**, *126*, 218002.
(67) Yu, A. C.; Lian, H.; Kong, X.; Lopez Hernandez, H.; Qin, J.; Appel, E. A. Physical Networks from Entropy-Driven Non-Covalent Interactions. *Nat. Commun.* **2021**, *12*, 746.
(68) Mason, T. G.; Bibette, J.; Weitz, D. A. Elasticity of Compressed Emulsions. *Phys. Rev. Lett.* **1995**, *75*, 2051−2054.

https://doi.org/10.1021/acsmacrolett.4c00428
ACS Macro Lett. 2024, 13, 1304−1310

(69) Koumakis, N.; Schofield, A. B.; Petekidis, G. Effects of Shear Induced Crystallization on the Rheology and Ageing of Hard Sphere Glasses. *Soft Matter* **2008**, *4*, 2008.
(70) McLeish, T. C. B. Tube Theory of Entangled Polymer Dynamics. *Adv. Phys.* **2002**, *51*, 1379−1527.
(71) Rubinstein, M.; Colby, R. H. *Polymer Physics*; Oxford University Press, 2003.
(72) McCrum, N. G.; Buckley, C. P.; Bucknall, C. B. *Principles of Polymer Engineering*, 1:2 ed.; Oxford Univ. Press: Oxford, 2010.
(73) Grunlan, J. C.; Gerberich, W. W.; Francis, L. F. Lowering the Percolation Threshold of Conductive Composites Using Particulate Polymer Microstructure. *J. Appl. Polym. Sci.* **2001**, *80*, 692−705.
(74) Ram, R.; Rahaman, M.; Aldalbahi, A.; Khastgir, D. Determination of Percolation Threshold and Electrical Conductivity of Polyvinylidene Fluoride (PVDF)/Short Carbon Fiber (SCF) Composites: Effect of SCF Aspect Ratio. *Polym. Int.* **2017**, *66*, 573−582.
(75) Choi, H.-J.; Kim, M. S.; Ahn, D.; Yeo, S. Y.; Lee, S. Electrical Percolation Threshold of Carbon Black in a Polymer Matrix and Its Application to Antistatic Fibre. *Sci. Rep.* **2019**, *9*, 6338.
(76) Gouveia, M.; Dias, C. S.; Tavares, J. M. Percolation in Binary Mixtures of Linkers and Particles: Chaining vs Branching. *J. Chem. Phys.* **2022**, *157*, 164903.
(77) Bolhuis, P. G.; Meijer, E. J.; Louis, A. A. Colloid-Polymer Mixtures in the Protein Limit. *Phys. Rev. Lett.* **2003**, *90*, 068304.
(78) Lu, P. J.; Zaccarelli, E.; Ciulla, F.; Schofield, A. B.; Sciortino, F.; Weitz, D. A. Gelation of Particles with Short-Range Attraction. *Nature* **2008**, *453*, 499−503.
(79) Lekkerkerker, H. N.; Tuinier, R. *Colloids and the Depletion Interaction*; Springer: Netherlands; Dordrecht, 2011; Vol. *833*.
(80) Gam, S.; Meth, J. S.; Zane, S. G.; Chi, C.; Wood, B. A.; Winey, K. I.; Clarke, N.; Composto, R. J. Polymer Diffusion in a Polymer Nanocomposite: Effect of Nanoparticle Size and Polydispersity. *Soft Matter* **2012**, *8*, 6512.
(81) Zhou, H.; Schön, E.-M.; Wang, M.; Glassman, M. J.; Liu, J.; Zhong, M.; Díaz Díaz, D.; Olsen, B. D.; Johnson, J. A. Crossover Experiments Applied to Network Formation Reactions: Improved Strategies for Counting Elastically Inactive Molecular Defects in PEG Gels and Hyperbranched Polymers. *J. Am. Chem. Soc.* **2014**, *136*, 9464−9470.
(82) Ye, Y. N.; Cui, K.; Indei, T.; Nakajima, T.; Hourdet, D.; Kurokawa, T.; Gong, J. P. Relaxation Dynamics and Underlying Mechanism of a Thermally Reversible Gel from Symmetric Triblock Copolymer. *Macromolecules* **2019**, *52*, 8651−8661.
(83) Pozzo, D. C.; Walker, L. M. Reversible Shear Gelation of Polymer-Clay Dispersions. *Colloid Surface A* **2004**, *240*, 187−198.
(84) Matsen, M. W. Bridging and Looping in Multiblock Copolymer Melts. *J. Chem. Phys.* **1995**, *102*, 3884−3887.
(85) Watanabe, H. Slow Dielectric Relaxation of a Styrene-Isoprene-Styrene Triblock Copolymer with Dipole Inversion in the Middle Block: A Challenge to a Loop/Bridge Problem. *Macromolecules* **1995**, *28*, 5006−5011.
(86) Ryu, C. Y.; Ruokolainen, J.; Fredrickson, G. H.; Kramer, E. J.; Hahn, S. F. Chain Architecture Effects on Deformation and Fracture of Block Copolymers with Unentangled Matrices. *Macromolecules* **2002**, *35*, 2157−2166.
(87) Mori, Y.; Lim, L. S.; Bates, F. S. Consequences of Molecular Bridging in Lamellae-Forming Triblock/Pentablock Copolymer Blends. *Macromolecules* **2003**, *36*, 9879−9888.
(88) Phatak, A.; Lim, L. S.; Reaves, C. K.; Bates, F. S. Toughness of Glassy-Semicrystalline Multiblock Copolymers. *Macromolecules* **2006**, *39*, 6221−6228.
(89) Spakowitz, A. J.; Wang, Z.-G. End-to-End Distance Vector Distribution with Fixed End Orientations for the Wormlike Chain Model. *Phys. Rev. E* **2005**, *72*, 041802.
(90) Sunday, D. F.; Chang, A. B.; Liman, C. D.; Gann, E.; Delongchamp, D. M.; Thomsen, L.; Matsen, M. W.; Grubbs, R. H.; Soles, C. L. Self-Assembly of ABC Bottlebrush Triblock Terpolymers with Evidence for Looped Backbone Conformations. *Macromolecules* **2018**, *51*, 7178−7185.
(91) Wei, P.; Cipriani, C.; Hsieh, C.-M.; Kamani, K.; Rogers, S.; Pentzer, E. Go with the Flow: Rheological Requirements for Direct Ink Write Printability. *J. Appl. Phys.* **2023**, *134*, 100701.
(92) Kratochvil, M. J.; Seymour, A. J.; Li, T. L.; Paşca, S. P.; Kuo, C. J.; Heilshorn, S. C. Engineered Materials for Organoid Systems. *Nat. Rev. Mater.* **2019**, *4*, 606−622.

https://doi.org/10.1021/acsmacrolett.4c00428
ACS Macro Lett. 2024, 13, 1304−1310